| human reproduction | **ORIGINAL ARTICLE** *Reproductive biology* |

The cyto-protective effects of LH on ovarian reserve and female fertility during exposure to gonadotoxic alkylating agents in an adult mouse model

L.M. Del Castillo[1,2], A. Buigues[1], V. Rossi[3], M.J. Soriano[1], J. Martinez[1,2], M. De Felici[3], H.K. Lamsira[3], F. Di Rella[4], F.G. Klinger[3], A. Pellicer[1,5], and S. Herraiz ⃝[1,*]

[1]IVI Foundation—IIS La Fe, Reproductive Medicine Research Group, Valencia, Spain [2]Department of Pediatrics, Obstetrics and Gynecology, School of Medicine, University of Valencia, Valencia, Spain [3]Department of Biomedicine and Prevention, University of Rome Tor Vergata, Rome, Italy [4]Clinical and Experimental Senology, Istituto Nazionale Tumori, IRCCS, Fondazione G. Pascale, Naples, Italy [5]IVI-RMA Rome, Rome, Italy

*Correspondence address. IVI Foundation—IIS La Fe, Reproductive Medicine Research Group, Av. Fernando Abril Martorell, 106-Torre A-Planta1, 46026 Valencia, Spain. Tel: +34-96-390-33-05; E-mail: Sonia.Herraiz@ivirma.com ⃝ https://orcid.org/0000-0003-0703-6922

STUDY QUESTION: Does LH protect mouse oocytes and female fertility from alkylating chemotherapy?

SUMMARY ANSWER: LH treatment before and during chemotherapy prevents detrimental effects on follicles and reproductive lifespan.

WHAT IS KNOWN ALREADY: Chemotherapies can damage the ovary, resulting in premature ovarian failure and reduced fertility in cancer survivors. LH was recently suggested to protect prepubertal mouse follicles from chemotoxic effects of cisplatin treatment.

STUDY DESIGN, SIZE, DURATION: This experimental study investigated LH effects on primordial follicles exposed to chemotherapy. Seven-week-old CD-1 female mice were randomly allocated to four experimental groups: Control (n = 13), chemotherapy (ChT, n = 15), ChT+LH-1x (n = 15), and ChT+LH-5x (n = 8). To induce primary ovarian insufficiency (POI), animals in the ChT and ChT+LH groups were intraperitoneally injected with 120 mg/kg of cyclophosphamide and 12 mg/kg of busulfan, while control mice received vehicle. For LH treatment, the ChT+LH-1x and ChT+LH-5x animals received a 1 or 5 IU LH dose, respectively, before chemotherapy, then a second LH injection administered with chemotherapy 24 h later. Then, two animals/group were euthanized at 12 and 24 h to investigate the early ovarian response to LH, while remaining mice were housed for 30 days to evaluate short- and long-term reproductive outcomes. The effects of LH and chemotherapy on growing-stage follicles were analyzed in a parallel experiment. Seven-week-old NOD-SCID female mice were allocated to control (n = 5), ChT (n = 5), and ChT+LH-1x (n = 6) groups. Animals were treated as described above, but maintained for 7 days before reproductive assessment.

PARTICIPANTS/MATERIALS, SETTING, METHODS: In the first experiment, follicular damage (phosphorylated H2AX histone (γH2AX) staining and terminal deoxynucleotidyl transferase-mediated dUTP nick-end labeling (TUNEL) assay), apoptotic biomarkers (western blot), and DNA repair pathways (western blot and RT-qPCR) were assessed in ovaries collected at 12 and 24 h to determine early ovarian responses to LH. Thirty days after treatments, remaining mice were stimulated (10 IU of pregnant mare serum gonadotropin (PMSG) and 10 IU of hCG) and mated to collect ovaries, oocytes, and embryos. Histological analysis was performed on ovarian samples to investigate follicular populations and stromal status, and meiotic spindle and chromosome alignment was measured in oocytes by confocal microscopy. Long-term effects were monitored by assessing pregnancy rate and litter size during six consecutive breeding attempts. In the second experiment, mice were stimulated and mated 7 days after treatments and ovaries, oocytes, and embryos were collected. Follicular numbers, follicular protection (DNA damage and apoptosis by H2AX staining and TUNEL assay, respectively), and ovarian stroma were assessed. Oocyte quality was determined by confocal analysis.

MAIN RESULTS AND THE ROLE OF CHANCE: LH treatment was sufficient to preserve ovarian reserve and follicular development, avoid atresia, and restore ovulation and meiotic spindle configuration in mature oocytes exposed at the primordial stage. LH improved the cumulative pregnancy rate and litter size in six consecutive breeding rounds, confirming the potential of LH treatment to preserve fertility. This protective effect appeared to be mediated by an enhanced early DNA repair response, via homologous recombination, and generation of anti-apoptotic signals in the ovary a few hours after injury with chemotherapy. This response ameliorated the chemotherapy-induced increase in DNA-damaged oocytes and apoptotic granulosa cells. LH treatment also protected growing follicles from chemotherapy. LH reversed the chemotherapy-induced depletion of primordial and primary follicular subpopulations, reduced oocyte DNA damage and granulosa cell apoptosis, restored mature oocyte cohort size, and improved meiotic spindle properties.

LARGE SCALE DATA: N/A.

LIMITATIONS, REASONS FOR CAUTION: This was a preliminary study performed with mouse ovarian samples. Therefore, preclinical research with human samples is required for validation.

WIDER IMPLICATIONS OF THE FINDINGS: The current study tested if LH could protect the adult mouse ovarian reserve and reproductive lifespan from alkylating chemotherapy. These findings highlight the therapeutic potential of LH as a complementary non-surgical strategy for preserving fertility in female cancer patients.

STUDY FUNDING/COMPETING INTEREST(S): This study was supported by grants from the Regional Valencian Ministry of Education (PROMETEO/2018/137), the Spanish Ministry of Science and Innovation (CP19/00141), and the Spanish Ministry of Education, Culture and Sports (FPU16/05264). The authors declare no conflict of interest.

Key words: fertility preservation / follicle protection / ovoprotection / cancer / chemotherapy / LH / DNA repair

Introduction

The female reproductive lifespan is widely thought to depend on the number of non-renewable primordial follicles, constituting the ovarian reserve that progressively decreases with age (Macklon and Fauser, 1999). External factors, such as chemotherapy treatment, can accelerate follicular depletion and menopause onset. Cytotoxic treatments cause a spectrum of effects on the ovary ranging from partial damage, to premature ovarian insufficiency (POI) and loss of fertility (Koyama et al., 1977; Kalich-Philosoph et al., 2013; Spears et al., 2019). Notably, oncologic treatments cause a 38% reduction in the likelihood that patients will achieve pregnancy (Anderson et al., 2018).

This is a growing problem worldwide, with over 1.9 million women of reproductive age (15–49 years old) newly diagnosed with cancer in 2018 alone (Ferlay et al., 2018). Among young women who are nulliparous, the 5-year cancer survival rate can be as high as 75% (Howlader et al., 2019). Thus, a growing number of female patients will experience the undesired gonadotoxic side effects associated with oncologic treatments, highlighting the relevance of fertility preservation.

Patient age and type and dose of chemotherapeutic agent are the main factors determining the degree of ovarian damage (Kalich-Philosoph et al., 2013), with older patients being more susceptible to POI after treatment. Among chemotherapeutic drugs, alkylating agents, like cyclophosphamide and busulfan, associate with the highest risk of inducing follicular depletion leading to POI (Meirow et al., 2010). Although the precise mechanism for follicle depletion by alkylating agents remains unclear, these cytotoxic drugs derive their anticancer properties by inducing inter- and intra-strand DNA crosslinking that leads to apoptosis and cell death.

The ability to respond to DNA insults is critical to ensure follicular viability. In meiotic cells (e.g. oocytes), homologous recombination promoted by the ataxia telangiectasia-mutated pathway (ATM), is the primary mechanism for accurate double-strand break (DSB) repair (Kujjo et al., 2010; Kujjo et al., 2012; Winship et al., 2018).

Also, agents like cyclophosphamide damage growing follicles, thereby inducing the over-activation of dormant follicles, known as the burnout effect, that finally results in loss of the ovarian reserve (Kalich-Philosoph et al., 2013).

LH, a gonadotropin with a complex role in folliculogenesis, was recently proposed to protect the follicle pool of prepubertal mice from cisplatin. LH was proposed to prevent the chemotherapy-induced reduction of primordial follicles by stimulating anti-apoptotic signals from a subset of somatic cells expressing the LH receptor (LHR) (Rossi et al., 2017). Although these results are encouraging, further research is required because cisplatin only associates with a moderate risk of inducing POI (Meirow et al., 2010), and prepubertal ovaries lack late preantral and antral follicles, precluding evaluation of how over-activation contributes to follicular exhaustion. Furthermore, the developmental potential of LH-preserved oocytes and the underlying protective mechanisms remain unclear. We, thus, aimed to assess the effects of LH in protecting the adult mouse ovary, containing all follicle populations, from the most gonadotoxic alkylating agents. The competence of the LH-protected follicles was also analyzed.

Material and methods

Animal procedures

All animal experiments in this study were approved and performed according to the Institutional Review Board and the Ethics Committee in Experimental Research of the University of Valencia, Valencia, Spain (2018/VSC/PEA/0010 and 2019/VSC/PEA/0206).

Study design

This was an experimental study (study design summarized in Supplementary Fig. S1) to investigate LH effects on primordial follicles that were exposed to chemotherapy. Seven-week-old CD-1 female mice were randomly allocated to four experimental groups: Control

(n = 13), chemotherapy (ChT, n = 15), ChT+LH-1x (n = 15), and ChT+LH-5x (n = 8). Mice receiving chemotherapy were intraperitoneally injected with 120 mg/kg of cyclophosphamide and 12 mg/kg of busulfan in dimethyl sulfoxide (DMSO) (all from Sigma-Aldrich, St. Louis, Missouri, MO, USA), as previously described (Buigues et al., 2020), while controls were injected with saline. For LH treatments, the ChT+LH-1x and ChT+LH-5x mice were dosed with 1 (2.3 ng/ml) or 5 (11.5 ng/ml) IU of LH (Luveris, Merck Serono, Darmstadt, Germany), respectively, before chemotherapy and then again with chemotherapy 24 h later. After treatments, the early ovarian response to LH and both the short- and long-term reproductive outcomes were assessed.

In a parallel experiment to analyze LH effects on growing follicles exposed to chemotherapy, 7-week-old NOD-SCID female mice were allocated to control (n = 5), ChT (n = 5), and ChT+LH-1x (n = 6) groups. Mice were treated as described above and maintained for 7 days.

Effects on quiescent follicles
To evaluate the LH effects on follicles at the dormant primordial stage during chemotherapy exposure (Supplementary Fig. S1A), 31 seven-week-old CD-1 female mice randomly allocated to control, chemotherapy (ChT) and chemotherapy with LH (ChT+LH-1x) groups and treated as described above were maintained for 30 days. These mice were then subjected to controlled ovarian stimulation (COS) to recover oocytes and embryos derived from follicles damaged at the primordial stage. Two mice from each group were euthanized 16 h after hCG administration to collect mature oocytes, while the remaining were housed with males immediately after hCG injection and euthanized 40 h later to collect ovaries, oocytes, and early cleavage-stage embryos. To assess the long-term effects of LH, 30 days after treatments 4 mice/group were housed with fertile males for 6 months to allow continuous breeding. For long-term assessment, an additional group treated with a high-dose, i.e. 5 IU, of LH (11.5 ng/ml) was included (ChT+LH-5x).

To analyze the protective early response to LH, a complementary experiment was performed on 16 CD-1 female mice treated with LH and alkylating agents as described above and euthanized 12 and 24 h after ChT and/or LH treatment to evaluate ovarian samples (Supplementary Fig. S1B).

An *in vivo* experiment was performed with cisplatin to determine if the protective effects of LH depended on the type of chemotherapy agent. Twenty-four 7-week-old CD-1 female mice were allocated to four experimental groups (n = 6/group): control, cisplatin (Cs), LH, and cisplatin with LH (Cs+LH). Mice received a single dose of 5 mg/kg of cisplatin, 1 IU of LH, or saline solution as a control. The fourth group received 1 IU of LH together with 5 mg/kg of cisplatin. Ovaries were collected 5 days after treatment to count follicles.

Effects on growing oocyte populations
Finally, to test if LH can also protect the growing follicle population, NOD/SCID female mice were used. These mice represent a worst-case ovarian scenario as they are considerably less fertile than the CD-1 strain (Kumagai et al., 2011). Sixteen 7-week-old NOD-SCID female mice were randomly allocated to control, ChT, and ChT+LH-1x groups, and treatments administered as described above. Seven days after treatment, mice underwent COS to ensure that any collected

oocytes were derived from growing-stage follicles exposed to chemotherapy. Two mice per group were euthanized 16 h after hCG injection to collect oocytes, while remaining mice were mated with males immediately after hCG injection and euthanized 40 h later to collect ovaries, metaphase II (MII) ovulated oocytes, and early cleavage-stage embryos from oviducts (Supplementary Fig. S1C).

Histological evaluation and follicle count
Formalin-fixed ovarian samples were paraffin-embedded and cut into 4-μm thick sections. Every fifth section was stained with hematoxylin and eosin (H&E) for morphological evaluation and follicle count. Follicular counts were performed blindly by three observers (L.M.C., A.B., and J.M.), and only follicles with a visible nucleus were counted to avoid double counting. Developmental stages were classified according to standard criteria (Dath et al., 2010). The following follicles were considered morphologically abnormal: presence of two or more oocytes in the same follicle, multiple vesicles on ooplasm, disruption of granulosa layers, or complete degeneration (Supplementary Fig. S2). Stromal degeneration was assessed over the whole ovary in representative H&E sections with a bright-field microscope, identified as the presence of fibrotic non-cellular or tissue absent regions embedded in ovarian stroma. A degenerated area index was quantified as the disrupted area/total tissue area of each sample using ImageJ software (National Institutes of Health, Bethesda, MD, USA). For each treatment group, mean stromal degeneration indices were calculated, normalized to the index of the control group, and expressed as fold-changes.

Oocytes and early cleavage-stage embryo collection
Dissected reproductive tracts were placed in a small petri dish containing flushing media (Origio, Måløv, Denmark) at 37°C and oviducts carefully isolated by removing ovaries and uteri with a sterilized blade. Oocytes and embryos were flushed from the oviducts by expelling flushing media from a 30-gauge needle inserted into the infundibulum. To determine an oocyte's maturation stage, cumulus–oocyte complexes were denuded with 300 μg/ml hyaluronidase (Sigma-Aldrich) for 30–60 s. Oocytes and embryos were classified according to morphological criteria under a binocular loupe (SZX2, Olympus, Tokyo, Japan).

Meiotic spindle staining and chromosome assessment
MII-oocytes obtained 16 h after hCG administration from CD-1 (n = 33) and NOD-SCID (n = 28) mice were processed and stained according to Coticchio et al. (2013) with minor modifications. Briefly, for microtubule and centromere staining, fixed oocytes were incubated with anti μ-Tubulin conjugated with fluorescein isothiocyanate (FITC) (1:50 dilution; F2168—Sigma-Aldrich) and anti-centromere proteins (CREST, 1:20 dilution; 15-234—Antibodies Incorporated, Davis, CA, USA) primary antibodies overnight at 4°C inside a dark humidified chamber. Then, oocytes were incubated with an Alexa Fluor 594 secondary antibody (1:1000 dilution; A-11014—Invitrogen, Carlsbad, CA, USA) for 1 h at room temperature (RT). Chromosomes were labeled using 20 μg/ml Hoechst fluorescent stain (H33342—Sigma-Aldrich) for

20 min at RT. High-resolution images were captured with a confocal microscope (Leica TCS SP8, Leica Microsystems GmbH, Wetzlar, Germany) and LAS X image software (Leica Microsystems GmbH). Total spindle areas and chromosome alignments were analyzed for each oocyte using ImageJ software (National Institutes of Health). Oocytes were classified as misaligned when at least one chromosome diverged by $\geq 2\,\mu m$ from the equatorial plate as previously described (Coticchio et al., 2013).

Cell damage

DNA damage and apoptosis in follicles were examined by immunofluorescence for phosphorylated H2AX histone (γH2AX), a specific marker of DSBs, and by terminal deoxynucleotidyl transferase-mediated dUTP nick-end labeling (TUNEL) assay, respectively. For γH2AX immunostaining, samples were incubated overnight at 4°C with a monoclonal rabbit anti-γH2AX antibody (1:400 dilution; 9718—Cell Signaling, Danvers, MA, USA) followed by a 1 h incubation at RT with a biotinylated goat anti-rabbit IgG secondary antibody (1:500 dilution; BA-1000—Vector Laboratories, Burlingame, CA, USA). Fluorescence staining was performed using streptavidin-conjugated Alexa Fluor 594 (1:1000 dilution; S32356—Invitrogen) for 45 min at RT. Samples were mounted with Fluoroshield mounting medium with DAPI (Abcam, Cambridge, UK). For TUNEL assay, DNA fragmentation was assessed by a TMR red in situ cell death detection kit (Roche Diagnostics, Basel, Switzerland), following the manufacturer's instructions.

Stained sections were examined and high-magnification images obtained using a fluorescence microscope with an attached digital camera (Leica DM4000B and DFC450C, Leica Microsystems GmbH). Oocytes containing positive γH2AX-labeled foci were considered damaged, and the DNA damage index calculated as γH2AX-positive/total oocytes for each sample. TUNEL-positive labelling was quantified by Image ProPlus 6.0 software (Media Cybernetics Inc., Rockville, MD, USA), and follicles were considered apoptotic when showing $\geq 20\%$ TUNEL-positive granulosa cells.

Western blotting

Frozen ovaries were homogenized in RIPA lysis buffer (50 mM Tris-HCl, 150 mM NaCl, 4% NP-40, 0.5% sodium deoxycholate, 0.1% sodium dodecyl sulfate (SDS), pH 7.4) containing phosphatase (PhospSTOP EASYpack, Roche Diagnostics) and protease (cOmplete tablets EDTA-free EASY-pack, Roche Diagnostics) inhibitors. Protein content was determined by Bradford assay. Subsequently, 30 µg of protein from each sample were separated on 8–12% SDS-polyacrylamide gels and transferred to polyvinylidene difluoride (PVDF) membranes. Blots were blocked using 5% bovine serum albumin (BSA, Sigma-Aldrich) or non-fat powdered milk dissolved in Tris-Buffered saline with 0.1% Tween 20 (TBST) for 1 h at RT and then exposed to primary antibodies—ataxia-telangiectasia mutated kinase (ATM, 1:2000 dilution; ab78), RAD51 recombinase (Rad51, 1:5000 dilution; ab133534—both from Abcam), cleaved Caspase-3 (CC3, 1:1000 dilution; 9661), phospho-extracellular signal-regulated Kinase 1 and 2 (pERK1/2, 1:1000 dilution; 4370), ERK1/2 (1:1000 dilution; 4695), phospho- serine/threonine-protein Kinase 1 (pAkt, 1:1000 dilution; 4060), Akt (1:500 dilution; 4691—all five from Cell Signaling), B-cell lymphoma-2 (Bcl2, 1:200 dilution; sc7382) or β-Actin (1:2000 dilution;

sc47778—both from Santa Cruz Biotechnology, Dallas, TX, USA)—overnight at 4°C. After washing in TBST, membranes were incubated with appropriate Horseradish peroxidase (HRP)-conjugated secondary antibodies for 1 h at RT. Following incubation with a chemiluminescence detection reagent (ThermoFisher, Waltham, MA, USA), protein bands were visualized by Amersham Imager 680 (GE HealthCare Life Sciences, Marlborough, MA, USA). Integrated light intensity of each band was determined by ImageJ software (National Institutes of Health). Signal intensities were normalized to the intensity of the housekeeping protein β-Actin.

Relative gene expression

Total RNA was obtained from ovaries collected 12 and 24 h after chemotherapy administration using the RNeasy micro kit (Qiagen, Hilden, Germany), according to the manufacturer's instructions, and complementary cDNA synthesized from 0.5 µg of RNA per sample using the PrimeScript RT reagent kit (Takara Bio Inc., Kusatsu, Japan). Real-time quantitative PCR (RT-qPCR) was performed with specific primers for DNA repair associated genes (Supplementary Table SI) using PoweUp Sybr Green (ThermoFisher) and a StepOnePlus system (Applied Biosystems, Foster City, CA, USA). All PCR reactions were run in triplicate, and the relative gene expression was calculated by the CT method (Livak and Schmittgen, 2001) using 18S ribosomal (Rn18s) as a housekeeping gene.

Statistics

Data are presented as mean and standard deviation (mean±SD). Sample size was estimated with R statistical programming language (pwr package; R Core Team, Vienna, Austria). Two-by-two comparisons between experimental groups were performed with the non-parametric Mann-Whitney test using SPSS v.22.0 (IBM, Chicago, IL, USA). For spindle assessment data, multiple comparisons between groups were performed using the Turkey all-pair comparisons method (multcomp R package) with the R statistical programming language. The spindle dichotomic variable (presence/absence) was analyzed by Bayesian analysis using a logistic regression and a normal non-informative prior (0 ± 3 as mean±SD). The quality of the Bayesian model was checked for 1000 simulations. Spindle area was analyzed by linear regression and the remaining variables by logistic regression. A P-value <0.05 was considered statistically significant.

Results

Protective effects of LH on quiescent follicles

Follicle endowment and ovarian stroma

Ovaries from mice treated with alkylating agents exhibited 69.8% ($P = 0.025$) fewer follicles than controls, particularly affecting the primordial, primary, and secondary populations ($P = 0.024$, $P = 0.025$ and $P = 0.034$, respectively; Fig. 1A and B). LH-treated samples had 53.8% fewer follicles than controls, but this difference was not statistically significant ($P = 0.063$, Fig. 1A). LH treatment ameliorated the chemotherapy-induced follicle loss and increased the number of primordial, primary, antral, and preovulatory follicles by 38.1%, 36.1%,
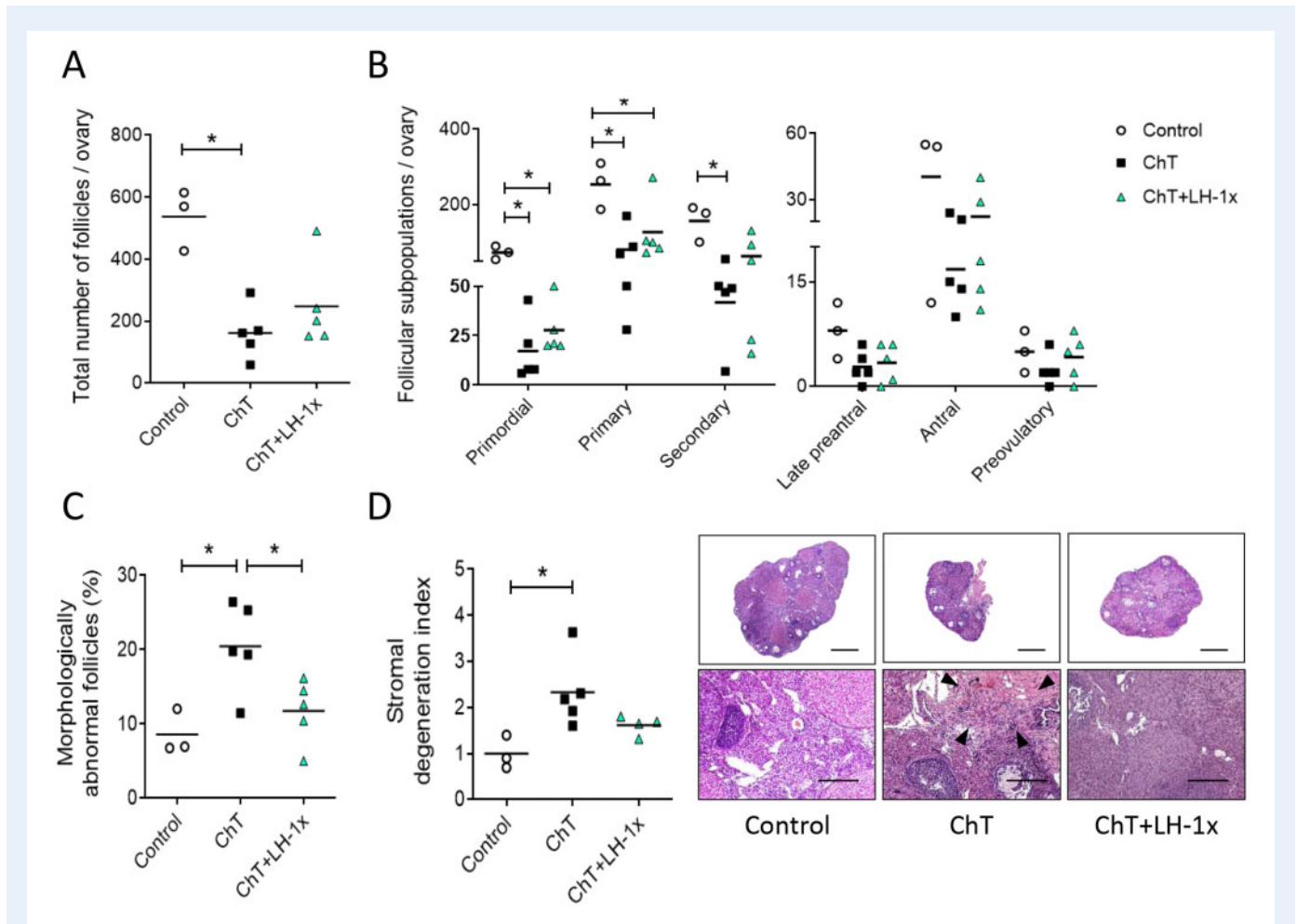
Figure 1. LH treatment prevented follicular depletion, atresia, and stromal degeneration induced by chemotherapy. Alkylating agents were administered with or without LH and ovaries analyzed 30 days later. (**A**) Chemotherapy (ChT) treatment reduced the number of total follicles assessed in hematoxylin and eosin (H&E) stained sections, and LH co-administration blunted this effect. (**B**) All follicular subpopulations were higher in the LH-cotreated group than in the ChT group. (**C**) Percentages of morphologically abnormal follicles were similar in the LH and control group, but the ChT group showed a significant increase in atretic follicles. (**D**) Stromal degeneration index (fibrotic non-cellular or tissue absent area/ total tissue area of each sample, normalized to control group index), and representative images at 2.5× (top, scale bar = 800 μm) and 10× (bottom, scale bar = 200 μm) magnification showing that LH preserves stromal morphology. Disrupted regions were identified as fibrotic areas and are indicated with black arrows in 10× images. Scatter plots show individual data and means for all groups (n = 3 in control and n = 5 in ChT and chemotherapy with LH (ChT+LH-1×) groups). Statistical significance was determined by two-tailed Mann–Whitney U test; *P-values <0.05 were considered statistically significant.

25.0%, and 52.4% of ChT follicle numbers, respectively, although these differences were not statistically significant due to high variability between samples. Relative to the control group, the ChT treatment group had more morphologically abnormal follicles ($P = 0.049$), while LH prevented this effect, with the LH group showing similar numbers of abnormal follicles as the control group and significantly fewer than the ChT group ($P = 0.047$; Fig. 1C).

ChT treatment also disrupted the structure of the ovarian stroma, with fibrotic areas localized in the center of the stroma being the most common alteration in ovaries from the ChT group. The mean stromal degeneration index of the ChT group was 2.3-fold higher than that of the control group ($P = 0.025$). Ovaries from the ChT+LH-1× group had well-preserved morphologies and exhibited only a slight 1.6-fold

increase in their stromal degeneration index relative to that of controls ($P = 0.077$; Fig. 1D). Thus, LH treatment blunted this chemotherapy-induced effect; albeit not statistically significant differences were found between ChT and ChT+LH-1× samples ($P = 0.086$).

Ovulation and early embryo cleavage
Relative to control mice, mice treated 30 days previously with alkylating agents yielded fewer MII-oocytes after COS ($P = 0.04$). LH treatment blunted this effect. The number of MII-oocytes collected from LH-treated mice was statistically similar ($P = 0.329$; Fig. 2A) to that of control mice and was 25.0% higher than that of ChT-treated mice. However, the ChT+LH-1× group had significantly fewer normal 2-cell embryos than the control group (Fig. 2B).
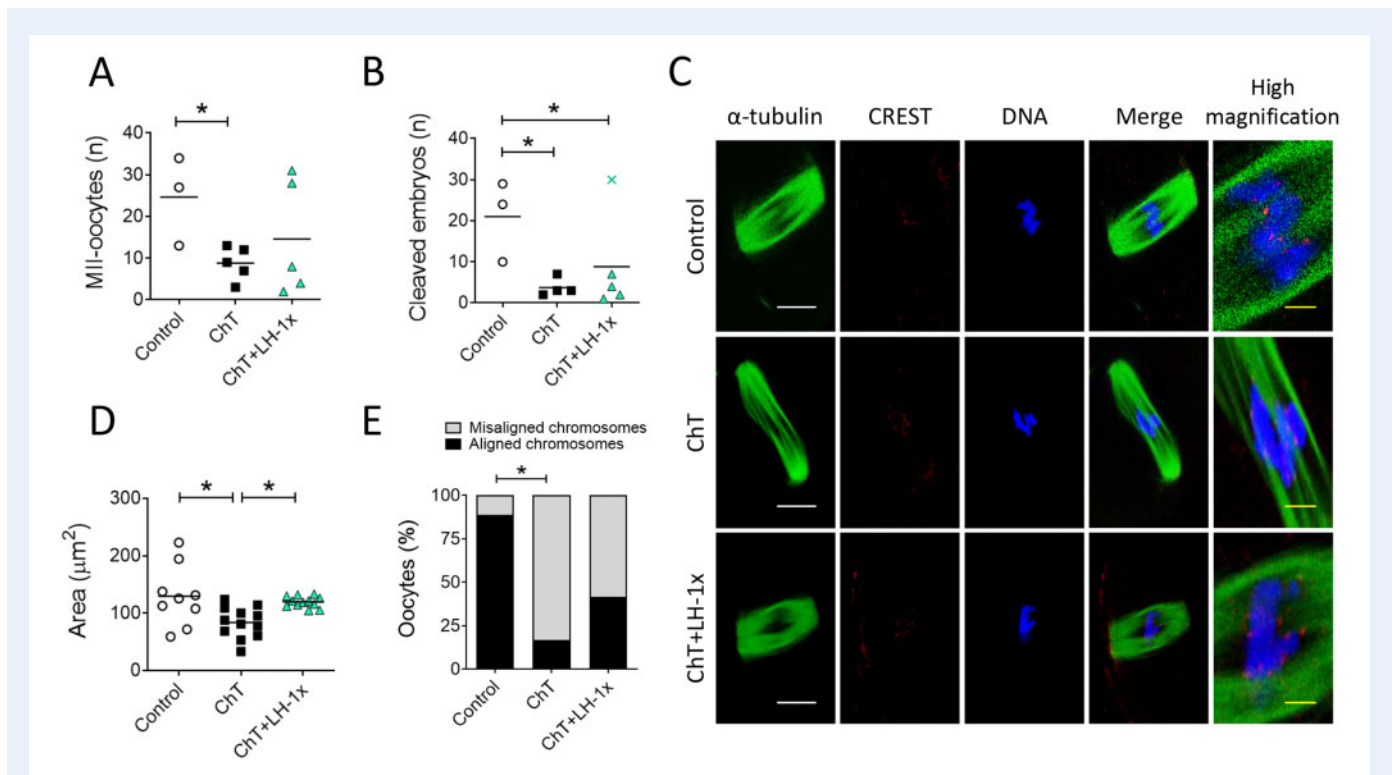
Figure 2. LH treatment ameliorated the effects of alkylators on oocyte quantity and quality. Alkylating agents were administered with or without LH and controlled ovarian stimulation (COS) performed 30 days later to release oocytes that had been exposed to chemotherapy during their quiescent stage. (**A**) Number of morphologically normal metaphase II (MII) oocytes recovered after COS from all experimental groups. LH-treated mice ovulated greater numbers of MII-oocytes than ChT-treated mice (**B**) Number of 2-cell stage embryos. (**C**) Representative confocal images of meiotic spindles from MII-oocytes (n = 9 in control, and n = 12 in ChT and in ChT+LH groups). α-tubulin staining (green) (showing spindles), chromosomes (blue), and CREST-centromere proteins (red) were visualized to evaluate chromosome alignment and microtubule–chromosome attachment. The right column shows high magnification images of merged optical sections. White scale bar = 10 μm; yellow scale bar = 1.25 μm. (**D**) Calculated spindle areas. LH treatment reversed the chemotherapy-induced reduction in spindle area. (**E**) Chromosomal alignment with reference to the metaphase plate. The LH-treated group had a lower percentage of misaligned chromosomes than the ChT group. Scatter plots indicate individual data and means of all analyzed mice (n = 5 in controls, and n = 7 in ChT and ChT+LH-1× groups). Outliers are indicated by a cross. Statistical significance was determined by two-tailed Mann–Whitney U test (A and B) or linear (D) and logistic (E) regressions; *P-values <0.05 were considered statistically significant.

Oocyte quality

Thirty-three MII-oocytes, all with meiotic spindles, were recovered from all experimental groups (Fig. 2C). The mean spindle area of oocytes from the ChT group was 35.3% less than the mean control spindle area ($P = 0.019$), but the mean spindle area of the LH-treated group was similar to that of controls and 31.1% higher than that of the ChT group ($P = 0.035$; Fig. 2D). Furthermore, the ChT group had more misaligned MII-oocytes than the control group ($P = 0.019$; Fig. 2E), and LH treatment ameliorated that effect, i.e. the number of misaligned MII oocytes were similar in the ChT+LH-1× and control groups.

Breeding trials

Reproductive lifespans of treated mice were assessed by breeding performance during six mating attempts (Fig. 3). As maternal age increased, pregnancy rates and litter sizes progressively decreased in all experimental groups. This decline was accelerated in the ChT group, with reduced cumulative pregnancy rate and litter size per delivery

(Fig. 3A–C) resulting in a 45.8% reduction in the number of live births relative to controls (Fig. 3D). In contrast, both LH-treated groups had better reproductive outcomes than the ChT group. In particular, the low-dose LH group had 21% more healthy pups than the ChT group.

The ovarian protective mechanism of LH

Twelve hours after chemotherapy treatment, DSBs were identified by γH2AX staining in oocytes at all follicular stages. All groups receiving chemotherapy had significantly higher percentages of γH2AX-positive oocytes than controls ($P = 0.034$ in all cases), but both the high and low LH-treated samples had significantly lower γH2AX expression levels than the ChT samples ($P = 0.021$ and $P = 0.020$, respectively, Fig. 4A). Growing follicles were the most affected population showing the highest percentage of γH2AX-positive oocytes after chemotherapy (Control: $22.4 \pm 1.8\%$, ChT: $69.4 \pm 13.6\%$, $P = 0.034$), although both LH dosages significantly reduced the chemotherapy-induced DNA damage (ChT+LH-1×: $45.7 \pm 4.8\%$, ChT+LH-5×: $39.4 \pm 5.7\%$; $P = 0.021$ in both cases).
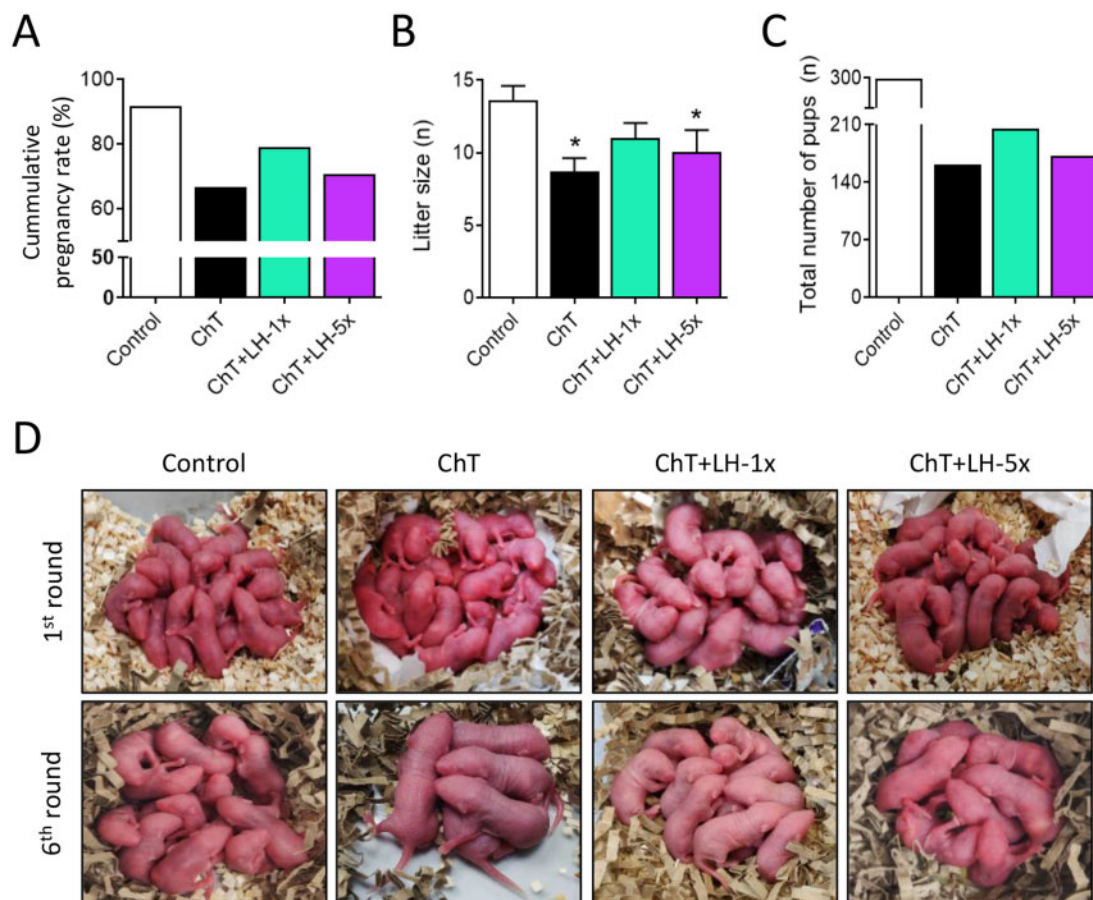
Figure 3. LH co-administration improved breeding outcomes and extended reproductive lifespan. Mice were treated with alkylating agents with or without LH and 1 month later tested for breeding performance in six consecutive mating attempts. (**A**) ChT (black) reduced the cumulative pregnancy rate and LH treatment reversed this, with the 1× dose (green) being more effective than the 5× dose (purple). (**B**) ChT reduced the mean litter size and LH-1× reversed this effect. (**C**) ChT reduced the total number of pups and LH-1×x ameliorated this effect. (**D**) Representative first and last litters from all experimental groups. Graphs show means and, where indicated, SD for each experimental group (n = 4 animals/group). Statistical significance for litter size was determined by two-tailed Mann–Whitney *U* test; *P-values <0.05 compared with the control group were considered statistically significant.

Twelve hours after treatment, there was an acute increase in the percent of apoptotic follicles (by TUNEL) in the ChT ($P = 0.034$) and ChT+LH-1× ($P = 0.034$) groups compared to controls. LH treatment protected ovaries from ChT-induced apoptosis in a dose-dependent manner, with a 1.6- and 6.7-fold reduction in apoptotic follicles in the ChT+LH-1× group ($P = 0.043$) and ChT+LH-5× ($P = 0.020$), respectively, when compared to the ChT group. The high-dose LH group had similar levels of apoptosis as controls (Fig. 4B). Growing follicles were the most susceptible population to apoptosis, but both the high and low doses of LH protected them from damage, resulting in a significantly lower TUNEL signal than that of the ChT group (Control: $2.0 \pm 1.7\%$, ChT: $10.3 \pm 1.6\%$, ChT+LH-1×: $5.6 \pm 2.1\%$ $P = 0.021$, ChT+LH-5×: $1.5 \pm 1.7\%$ $P = 0.020$). TUNEL-positive oocytes were not detected in any experimental group.

Additionally, the Bcl2/CC3 apoptosis protein ratio was similar in all groups (data not shown) twelve hours after treatments. However, at the 24 h timepoint the ChT group exhibited a reduction in the Bcl2/CC3 apoptosis protein ratio, and treatment with both high and low doses of LH restored this ratio to control-like levels (Fig. 4C and Supplementary Fig. S3A). Chemotherapy also increased ERK1/2 activation at both 12 and 24 h. Treatment with LH partially ameliorated this effect by reducing ERK1/2 phosphorylation (Fig. 4D and Supplementary Fig. S3B).

Finally, the high dose of LH increased the levels of the DNA DSB repair machinery ATM and Rad51 proteins (Fig. 4E and Supplementary Fig. S3C). Chemotherapy activated Akt, and treatment with both LH doses prevented this effect, reducing the pAkt/Akt ratio to control-like values at 12 and 24 h (Fig. 4F and Supplementary Fig. S3D). Chemotherapy also increased mRNA transcription of the DNA repair genes apurinic/apyrimidinic endodeoxyribonuclease 1 *(Apex1)*, mutS homolog 6 *(Msh6)*, protein kinase DNA-activated catalytic subunit *(Prkdc)*, excision repair cross-complementation group 3 *(Ercc3)*, and *Rad51* at the 12-h timepoint, which were downregulated by 24 h (Fig. 4G). Ovaries from ChT+LH-1×-treated mice showed an even more
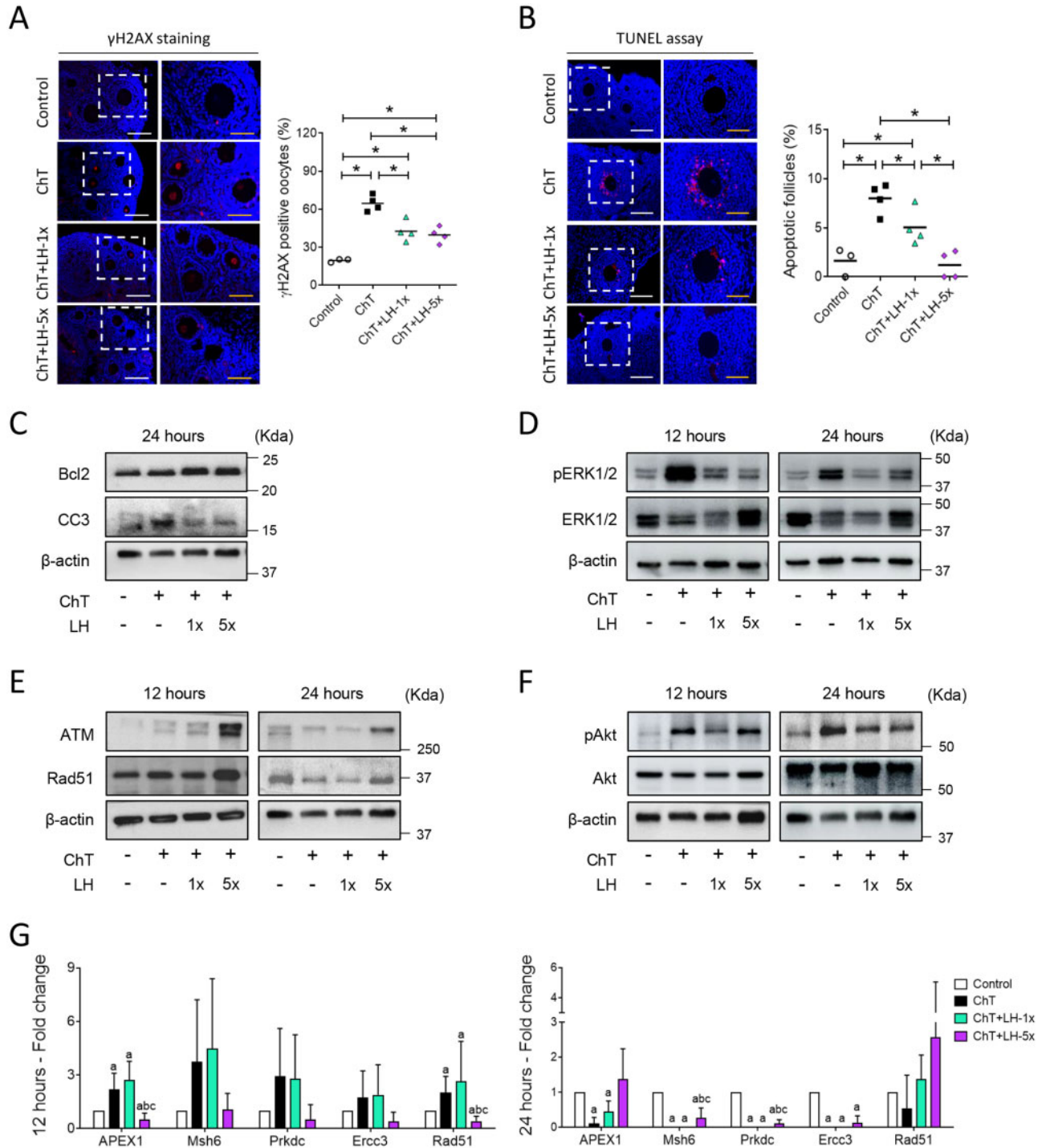
Figure 4. LH promoted DNA repair and cell survival and reduced the deleterious effects of chemotherapy on ovarian tissue.
Alkylating agents were administered with or without LH and ovaries assessed 12 and 24 h after (**A**) phosphorylated H2AX histone (γH2AX) immu-nofluorescence (red) counterstained with DAPI (blue) of ovarian samples collected 12 h after treatments with alkylating agents with or without a low (1×) or high (5×) dose of LH (n = 3 in controls, and n = 4 in ChT, ChT+LH-1×, and ChT+LH-5× groups). Images on the left are at 20× (white scale bar = 100 μm) and on the right at 40× (yellow scale bar = 50 μm). The percentages of follicles showing γH2AX positive oocytes were quanti-fied. The LH-treated groups had lower percentages of follicles with double-strand breaks (DSB) than the ChT group. (**B**) Terminal deoxynucleotidyl transferase-mediated dUTP nick-end labeling (TUNEL) assay (red) counterstained with DAPI (blue) was performed on ovarian sections 12 h after treatments. Magnifications and scale bars are as described in (A). Both LH-treated groups had a lower percentage of apoptotic follicles than the ChT group. (**C**) Representative western blots (WB) showing the levels of the anti-apoptotic protein B-cell lymphoma-2 (Bcl2) and the pro-apoptotic protein cleaved caspase-3 (CC3). Both doses of LH increased the Bcl2: CC3 ratio protecting the ovaries from ChT-induced cell death at 24 h.

robust upregulation of DNA repair genes, with expression of 4 out of 5 such genes reaching levels higher than that seen with ChT alone and with *Rad51* overexpression being maintained to 24 h. Unexpectedly, ChT+LH-5× ovaries showed an overall downregulation of DNA repair genes at both time-points, excepting *Rad51* at 24 h after treatment.

LH treatment protects ovaries from cisplatin

Cisplatin treatment similarly depleted the follicular pool by affecting all oocyte developmental stages (Supplementary Fig. S4). LH treatment prevented the cisplatin effects on the primordial and primary follicle populations, yielding 33.4% ($P = 0.041$) and 38.2% ($P = 0.009$) more follicles, respectively, than seen in the cisplatin-treated group.

Effects on growing follicles

LH treatment efficacy in a subfertile mouse model

We also assessed NOD-SCID mice, which are subfertile and therefore may provide a model for patients with aggressive cancers or already exhibiting reduced ovarian reserve. Here, NOD-SCID mice exhibited a 10-fold decrease of the follicular pool ($P = 0.050$; Fig. 5A) across all developmental stages (Fig. 5B) following chemotherapy. LH-treated ovaries contained 31.2% more follicles than the ChT-treated ovaries, with particular improvement in primordial and primary populations ($P = 0.034$ and $P = 0.032$, respectively). Indeed, the percentage of quiescent follicles in the ChT+LH-1× group was restored to control levels (Fig. 5C and D). Nevertheless, chemotherapy promoted follicular atresia, with increases in the number of morphologically abnormal follicles in both ChT and ChT+LH-1× ovaries compared to controls ($P = 0.050$ and $P = 0.034$, respectively; Fig. 5E). Furthermore, a 3.5-fold increase in the stromal degeneration index was detected in ChT samples ($P = 0.050$), while the increase in the ChT+LH-1× group was only 1.85-fold when referred to controls, indicating a reduction of the stromal negative effects seen in the ChT samples ($P = 0.047$; Fig. 5F).

Additionally, the ChT group had more γH2AX-positive oocytes (Fig. 5G) and TUNEL-positive follicles than controls ($P = 0.050$; Fig. 5H). However, LH treatment resulted in a lower percentage of DNA-damaged oocytes and a significant reduction in the percentage of apoptotic follicles ($P = 0.034$).

Chemotherapy also reduced the number of MII-oocytes ($P = 0.036$) and morphologically normal 2-cell embryos recovered after COS. However, the ChT+LH-1× group produced similar numbers of MII-oocytes as the control group and 26.3% more than the ChT group (Fig. 6A). This protective effect was not seen for 2-cell embryos (Fig. 6B).

Oocyte quality was then assessed in a total of 28 MII-oocytes. Meiotic spindle was only detected in 28.6% of MII-oocytes from the ChT group; in contrast and similar to the controls, all MII-oocytes from the ChT+LH-1× group contained a well-defined spindle (Fig. 6D). LH treatment increased the probability of proper spindle assembly by 60.9% relative to that of the ChT group (Fig. 6C). Chemotherapy also reduced the spindle area of MII-oocytes, with the spindle area of the ChT group being 5-fold lower than that of the control group ($P = 0.001$). A less severe, but still significant reduction in spindle area was also detected in oocytes from the LH-exposed group ($P = 0.030$, compared to controls). However, the LH-group exhibited a 3-fold increase in spindle area relative to that of the ChT group ($P = 0.049$; Fig. 6E). The ChT group also had more MII-oocytes with misaligned chromosomes than the control group ($P = 0.035$), but the ChT+LH-1× group had similar numbers as the controls and significantly fewer than the ChT group ($P = 0.029$; Fig. 6F).

Discussion

This study tested the effect of LH treatment on ovarian reserve in (i) quiescent follicles in CD-1 mice and (ii) growing follicles in NOD-SCID subfertile mice following chemotherapy with alkylating agents at a dose equivalent to that used in cancer patients (Grigg *et al.*, 2000). In the CD-1 model, LH prevented the negative effects of alkylating agents on ovarian reserve, follicular development, and oocyte quality and improved breeding performance. Further, LH treatment affected DNA repair pathways, suggesting these pathways may participate in the protective effects. Similar results were seen for growing follicles in the NOD-SCID model.

The effects of 1 IU of LH on both follicle count and MII-oocyte numbers four weeks after chemotherapy and LH treatment indicate that primordial follicles were the main target for the protective action of LH, since the timing is consistent with the window required for chemotherapy-exposed quiescent follicles to complete folliculogenesis (Clarke, 2017). This finding was confirmed in adult ovaries exposed to cisplatin, supporting previous observations in prepubertal mice (Rossi *et al.*, 2017) and indicating that LH can protect the ovarian reserve

---

Figure 4. Continued

(**D**) Representative WB showing phosphorylated-extracellular signal-regulated Kinase 1 and 2 (pERK1/2) and ERK1/2 protein levels. ChT activated ERK1/2 signaling and LH treatments reduced this effect at 12 and 24 h. (**E**) Representative WB for ataxia-telangiectasia mutated kinase (ATM) and RAD51 recombinase (Rad51) proteins. LH-5×-treated ovaries expressed higher levels of ATM and Rad51 than ChT-treated ovaries at 12 and 24 h. (**F**) Representative WB for phosphorylated-serine/threonine-protein Kinase 1 (pAkt) and Akt proteins. Chemotherapy caused a notable increase of Akt activation at both time-points, and cotreatment with LH blocked this effect. All WBs were performed from at least two independent experiments from two pools of two ovaries each per group. (**G**) mRNA expression levels of the indicated DNA repair genes at 12 (left) and 24 h (right). At 12 h, the expression levels of all repair genes were higher in the ChT+LH-1× samples than in the ChT samples. At 24 h, Rad51 expression was higher in both LH groups than in the ChT group. Three independent ovarian fragments per group and time-point was analyzed, and expression levels were normalized to those of the control group. Scatter plots indicate individual data and means; bar charts display means and SDs. Statistical significance was determined by two-tailed Mann–Whitney *U* test; *P*-values <0.05 were considered statistically significant. *$P < 0.05$ or [a]p <0.05, [b]P <0.05 and [c]P <0.05 indicating statistical differences from the control, ChT, and ChT+LH-1× group, respectively.
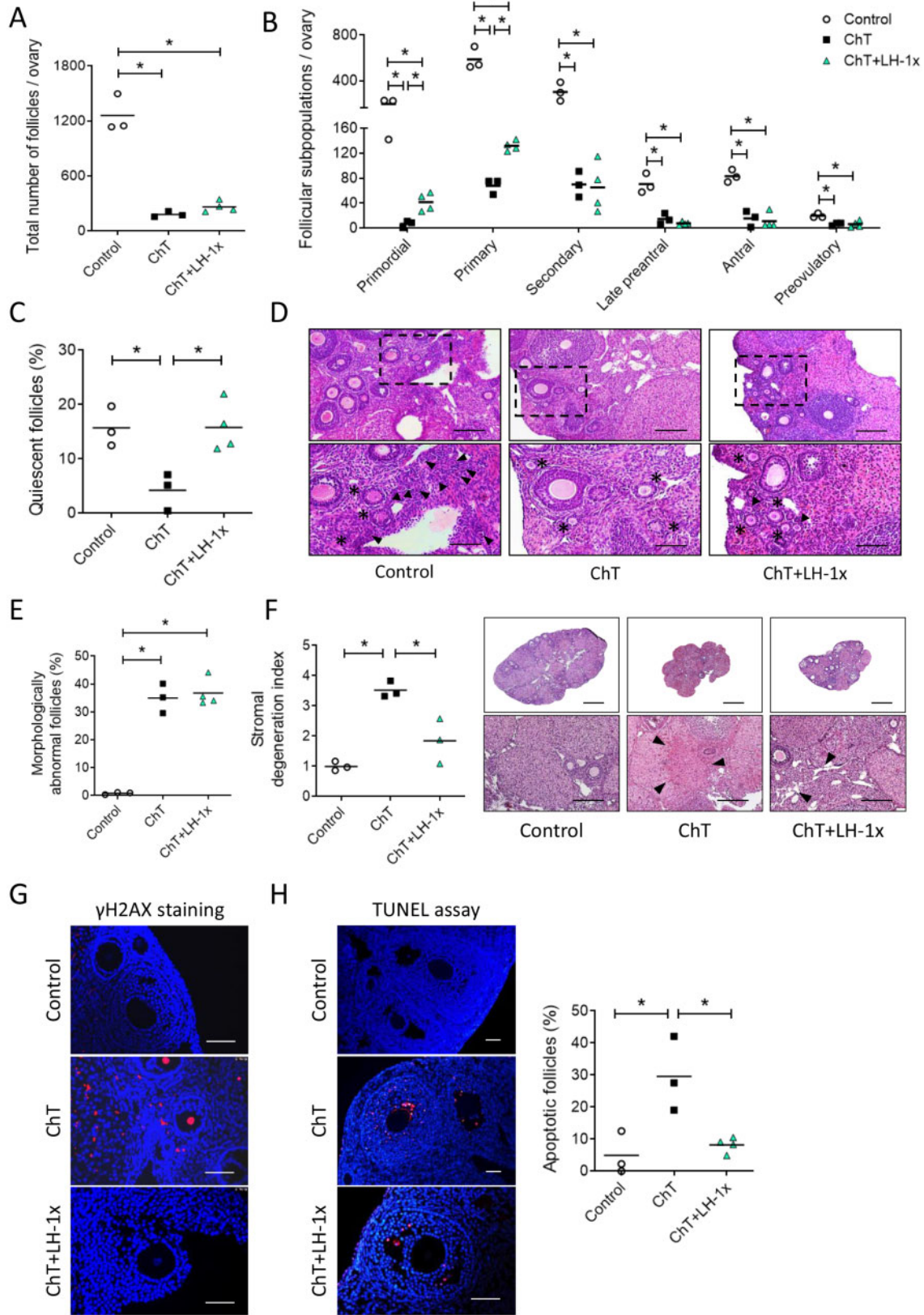
Figure 5. LH treatment protected the ovarian reserve and stromal architecture and prevented ChT-induced follicular damage in a subfertile NOD/SCID mouse model. Mice were treated with alkylating agents with or without LH and seven days later underwent COS. Ovaries were harvested and examined for follicle numbers, DNA damage, and apoptosis. (**A**) Total follicle numbers. (**B**) Follicle subpopulations.

from multiple types of agents. Consistent with previous studies (Petrillo *et al.*, 2011; Soleimani *et al.*, 2011; Luan *et al.*, 2019; Nguyen *et al.*, 2019; Wang, *et al.*, 2019), we observed a close relationship between follicle loss and oocyte damage followed by chemotherapy induced-cell death. Thus, the notable decrease of oocytes with γH2AX foci and apoptotic follicles observed 12 h after low- or high-dose LH suggests that DNA damage and cell death pathways mediate the preservative effect of LH on follicle counts.

DNA damage and apoptosis are intimately connected to cell fate determination in that cells with efficient DNA damage response or repair mechanisms are permitted to survive (Orren *et al.*, 1997; Biechonski *et al.*, 2018). In general, at both 12 and 24 h after treatment, ovaries from animals treated with LH had higher expression of DNA repair factors such as Rad51 than ovaries from animals treated with alkylating agents alone, indicating that LH stimulates DNA repair as previously suggested (Rossi *et al.*, 2017; Marcozzi *et al.*, 2019). In fact, overexpression of Rad51, a downstream target of the ATM pathway essential for the homologous recombination repair process, is a common mechanism by which cancer cells evade cytotoxic effects of oncologic therapies (Hu *et al.*, 2019) and follicular cells prevent apoptosis (Kujjo *et al.*, 2010, 2012). We also observed that LH treatment reduced Akt activation, a signaling pathway connecting DNA repair (Karimian *et al.*, 2019; Maidarti *et al.*, 2020) and DSB accumulation in primordial and primary follicles by inhibiting Rad51 (Shen *et al.*, 2007; Plo *et al.*, 2008; Maidarti *et al.*, 2019). Moreover, our findings suggested that LH decreases apoptosis by restoring CC3 levels, a specific cell death effector in oocytes and granulosa (Matikainen *et al.*, 2001; Takai *et al.*, 2007), and prevents ERK1/2 activation (Wei *et al.*, 2013; Rossi *et al.*, 2017).

MII meiotic spindle formation can serve as a measure of oocyte quality (Wang and Keefe, 2002; Rama *et al.*, 2007; Tomari *et al.*, 2018). We found that MII-oocytes that developed from primordial follicles exposed to chemotherapy exhibited defects in spindle area and chromosome alignment. Unrepaired DSBs in oocytes interfere with progression of the second meiotic division, proper spindle assembly, and chromosome cohesion (Watrin and Peters, 2006; Xiong *et al.*, 2008; Marangos *et al.*, 2015). Hence, the ability of LH to attenuate chemotherapy-induced DNA damage could underlie the improvements observed in spindle and chromosome alignment. Resting follicles were therefore protected by LH to preserve their subsequent development.

Bidirectional somatic-germ cell communication is crucial to generate a suitable microenvironment in the ovary and is required for oocyte competence and maturation. We found that chemotherapy affected the ovarian niche by degenerating the ovarian stroma and impairing oocyte maturation and quality, as previously reported (Zhang *et al.*, 2016; Wang *et al.*, 2019; Buigues *et al.*, 2020). However, treatment with LH reduced the deleterious effects on ovarian stromal cells and architecture. The protective LH effects on oocytes could occur, in part, via ovarian somatic cells that express the LH receptor (Chang *et al.*, 2015).

The short-term ability of LH to protect the ovarian reserve and improve the number and quality of developing oocytes appeared to translate into long-term benefits for reproductive performance. ChT-LH-treated mice had higher pregnancy rates and more pups than the ChT group, consistent with findings in cisplatin-treated mice (Rossi *et al.*, 2017). Interestingly, low-dose LH appeared to better preserve breeding performance. High LH dosage could adversely alter factors required for fertility, as previously described (Flaws *et al.*, 1997), and reported for some drugs (Bertoldo *et al.*, 2020; Park *et al.*, 2020). Administering gonadotropin-releasing hormone agonists (GnRHa) during chemotherapy can improve reproductive outcomes in oncologic patients (Blumenfeld *et al.*, 2015; Meli *et al.*, 2018; Sinha *et al.*, 2018), but their efficacy as gonadoprotective agents is controversial (Bildik *et al.*, 2015; Horicks *et al.*, 2018; Lambertini *et al.*, 2018; Sofiyeva *et al.*, 2019). The effects induced by our proposed LH treatment and the GnRHa therapies currently in use mainly differ in terms of treatment duration and cumulative dosage. We propose an acute administration of LH along with chemotherapy, but GnRHa therapies involve long-term repetitive treatments to achieve permanent suppression of the reproductive axis. Nevertheless, further research is needed to determine the best dosage and timing for LH during chemotherapy regimens.

When considering regimens to preserve fertility, a patient's ovarian pool is an important consideration. Patients with aggressive cancer and who have already received a chemotherapeutic cycle before undergoing fertility preservation are likely to already have diminished reserves and could benefit from therapies that can protect growing follicle populations. Using a mouse model with reduced fertility (NOD-SCID) (Kumagai *et al.*, 2011), we performed COS one week (instead of 4 weeks) after chemotherapy with or without LH treatment. LH significantly protected the most undifferentiated subpopulations (i.e.

Figure 5. Continued

The LH group had more total follicles than the ChT group. This effect was most appreciable in the primordial and primary populations, (**C**) ChT depleted the quiescent population and LH blocked this effect. (**D**) Representative H&E stained images captured at 10× (top, scale bar = 200 μm) and magnified images of the boxed regions at 20× (bottom, scale bar = 100 μm) showing primordial (black arrows) and primary (black asterisks) follicles. (E) LH treatment was unable to reverse the ChT-induced increase in the percentage of morphologically abnormal follicles. (**F**) Stromal degeneration index and representative images of lesions visualized at 2.5× (top, scale bar = 800 μm) and 10× (bottom, scale bar = 200 μm). Fibrotic areas are indicated with black arrows in 10x images. LH treatment protected ovaries from ChT-induced stromal degeneration. (**G**) Representative images of γH2AX (red) immunofluorescence counterstained with DAPI (blue). LH treatment protects cells from ChT-induced double-strand breaks. Scale bar = 100 μm. (**H**) Representative images of TUNEL-staining (red) counterstained with DAPI (blue). Scale bar = 50 μm. Apoptotic follicles ($\geq$ 20% labeled cells) were quantified. ChT treatment increased the percentage of apoptotic follicles, and LH treatment reversed this effect. Scatter plots indicate individual data and means of all analyzed mice (n = 3 in Control and ChT, and n = 4 in ChT+LH-1× groups). Statistical significance was determined by two-tailed Mann–Whitney *U* test; *P*-values <0.05 were considered statistically significant.
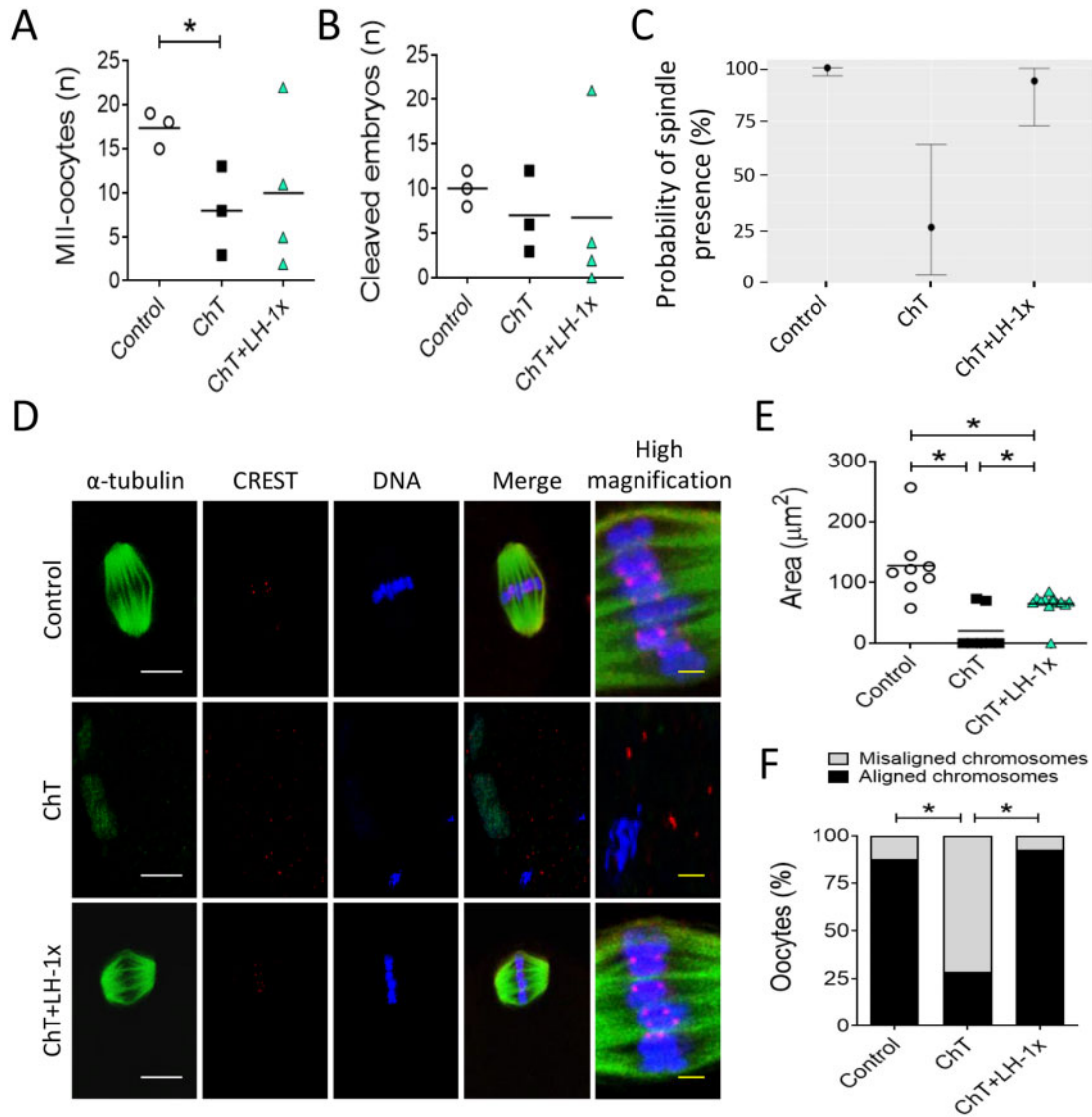
Figure 6. LH treatment ameliorated the effects of alkylators on oocyte quality in NOD/SCID mice. Mice were treated with alkylating agents with or without LH and 7 days later underwent COS to release oocytes that had been exposed to chemotherapy during their growth stage. (**A**) ChT reduced the number of healthy MII-oocytes ovulated after COS, and LH blunted this effect. (**B**) ChT decreased the number of early-cleavage stage embryos, and LH was unable to block this effect. (**C**) Bayesian model predicting the probability of spindle presence in MII-oocytes. LH treatment promoted spindle assembly during chemotherapy. (**D**) Representative images of meiotic spindles from ovulated MII-oocytes (n = 8 in Control, n = 7 in ChT, and n = 13 in ChT+LH-1× groups) and a high magnification view of the equatorial plate. α-tubulin staining (green), chromosomes (blue), and CREST-protein centromeres (red) were visualized. White scale bar = 10 μm; yellow scale bar = 1.25 μm. (**E**) Analysis of spindle area indicates LH treatment can ameliorate the effects of ChT. (**F**) Percentage of MII-oocytes with at least one misaligned chromosome as referred to the equatorial plate. ChT treatment resulted in a higher percentage of oocytes with misaligned chromosomes and LH treatment reversed this effect. Scatter plots indicated individual data and means of all analyzed mice (n = 5 in Control and ChT, and n = 6 in ChT+LH-1× groups). Statistical significance was determined by two-tailed Mann–Whitney U test (A and B), Bayesian analysis (C), linear (E) and logistic (F) regressions; *P-values <0.05 were considered statistically significant.

primordial and primary follicles), supporting both the results obtained in our first model and by other authors (Rossi et al., 2017). This effect may reflect reduced DNA damage in oocytes and/or diminished burnout effect (Kalich-Philosoph et al., 2013; Chang et al., 2015; Wang et al., 2019). Treatment with LH also blocked the deleterious effects of chemotherapy on growing oocyte populations, rescuing spindle defects and restoring suitable meiotic competence.

Altogether, these results indicate that, despite its short half-life (Santen and Bardin, 1973; Penny et al., 1977), LH is able to protect the ovary from alkylating agents. Cyclophosphamide and its active

metabolites have half-lives in plasma even shorter than that of LH (Powers and Sladek, 1983; Hong *et al.*, 1991; Rana *et al.*, 2007) but still trigger persistent cytotoxicity. Like cyclophosphamide, LH may trigger persisting effects by activating signaling pathways and cell functions.

LH and hCG have equivalent roles in clinical practice and can bind the same receptor; hCG has a longer half-life (Norman *et al.*, 2000), making it a strong candidate for gonadoprotection. However, LH and hCG differ in the amino acid residues required for binding to their shared receptor (Galet and Ascoli, 2005). This molecular variance leads to differing activities. LH is more effective as a proliferative and anti-apoptotic factor, while hCG has higher steroidogenic activity (Casarini *et al.*, 2016; Riccetti *et al.*, 2017). Nevertheless, hCG may be gonadoprotective, and further research should assess this.

In conclusion, this is the first study to analyze, in detail, the broad spectrum of protective effects elicited by LH on the ovarian reserve of adult mice during chemotherapy treatment with highly gonadotoxic agents. Mechanistically, LH appeared to prevent follicular depletion by reducing DNA damage in oocytes and by decreasing apoptosis and follicular atresia. We found that LH triggers an early DNA damage response after chemotherapy, which likely improves ovulation and oocyte competence. Treatment with LH also had long-term reproductive benefits, improving fertility and extending the reproductive lifespans of mice exposed to chemotherapy. Our research investigated LH effects using several approaches designed to represent different clinical reproductive scenarios, e.g. IVF cycles and natural conception, and uncovered possible mechanisms of action. Although these results were obtained in mice, the ability of LH to protect the mouse ovary from alkylating agents and cisplatin (Rossi *et al.*, 2017) highlights its therapeutic potential encouraging human clinical trials. Thus, a universal LH-based strategy may be possible for in situ ovarian reserve protection in female cancer patients.

Supplementary data

Supplementary data are available at *Human Reproduction* online.

Data availability

The data underlying this article will be shared on reasonable request to the corresponding author.

Acknowledgements

Authors' roles

L.M.C. conducted experimental studies, analyzed results, and wrote the manuscript; A.B. performed experiments and analyzed results; V.R., M.J.S., H.K.L., and J.M. contributed to performing the experiments; F.G.K., M.D.F., and F.D.R. designed and supervised the research and critically reviewed the manuscript; A.P. designed, supervised, coordinated, and funded the study and critically revised the manuscript; S.H. designed, coordinated, and conducted experiments, funded the research, and wrote the manuscript.

Funding

Conflict of interest

The authors declare no conflict of interest.

References

Anderson RA, Brewster DH, Wood R, Nowell S, Fischbacher C, Kelsey TW, Wallace WH. The impact of cancer on subsequent chance of pregnancy: a population based analysis. *Hum Reprod* 2018;**33**:1281–1290.

Bertoldo MJ, Listijono DR, Ho WHJ, Riepsamen AH, Goss DM, Richani D, Jin XL, Mahbub S, Campbell JM, Habibalahi A. *et al.* NAD+ repletion rescues female fertility during reproductive aging. *Cell Rep* 2020;**30**:1670–1681.

Biechonski S, Olender L, Zipin-Roitman A, Yassin M, Aqaqe N, Marcu-Malina V, Rall-Scharpf M, Trottier M, Meyn MS, Wiesmüller L. *et al.* Attenuated DNA damage responses and increased apoptosis characterize human hematopoietic stem cells exposed to irradiation. *Sci Rep* 2018;**8**:6071.

Bildik G, Akin N, Senbabaoglu F, Sahin GN, Karahuseyinoglu S, Ince U, Taskiran C, Selek U, Yakin K, Guzel Y. *et al.* GnRH agonist leuprolide acetate does not confer any protection against ovarian damage induced by chemotherapy and radiation in vitro. *Hum Reprod* 2015;**30**:2912–2925.

Blumenfeld Z, Zur H, Dann EJ. Gonadotropin-releasing hormone agonist cotreatment during chemotherapy may increase pregnancy rate in survivors. *Oncologist* 2015;**20**:1283–1289.

Buigues A, Marchante M, Herraiz S, Pellicer A. Diminished ovarian reserve chemotherapy-induced mouse model: a tool for the preclinical assessment of new therapies for ovarian damage. *Reprod Sci* 2020;**27**:1609–1619.

Casarini L, Riccetti L, De Pascali F, Nicoli A, Tagliavini S, Trenti T, La Sala GB, Simoni M. Follicle-stimulating hormone potentiates the steroidogenic activity of chorionic gonadotropin and the anti-apoptotic activity of luteinizing hormone in human granulosa-lutein cells in vitro. *Mol Cell Endocrinol* 2016;**422**:103–114.

Chang EM, Lim E, Yoon S, Jeong K, Bae S, Lee DR, Yoon TK, Choi Y, Lee W. Cisplatin induces overactivation of the dormant primordial follicle through PTEN/AKT/FOXO3α pathway which leads to loss of ovarian reserve in mice. *PLoS One* 2015;**10**:e0144245.

Clarke H. Control of mammalian oocyte development by interactions with the maternal follicular environment. *Results Probl Cell Differ* 2017;**63**:17–41.

Coticchio G, Guglielmo MC, Dal Canto M, Fadini R, Mignini Renzini M, De Ponti E, Brambillasca F, Albertini DF. Mechanistic

foundations of the metaphase II spindle of human oocytes matured in vivo and in vitro. *Hum Reprod* 2013;**28**:3271–3282.

Dath C, Van Eyck AS, Dolmans MM, Romeu L, Delle Vigne L, Donnez J, Van Langendonckt A. Xenotransplantation of human ovarian tissue to nude mice: comparison between four grafting sites. *Hum Reprod* 2010;**25**:1734–1743.

Ferlay J, Ervik J, Lam F, Colombet M, Mery L, Piñeros M, Znaor A, Soerjomataram BF. *Global Cancer Observatory: Cancer Today 2020*. Lyon, France: International Agency for Research on Cancer; 2018.

Flaws JA, Abbud R, Mann RJ, Nilson JH, Hirshfield AN. Chronically elevated luteinizing hormone depletes primordial follicles in the mouse ovary. *Biol Reprod* 1997;**57**:1233–1237.

Galet C, Ascoli M. The differential binding affinities of the luteinizing hormone (LH)/choriogonadotropin receptor for LH and choriogonadotropin are dictated by different extracellular domain residues. *Mol Endocrinol* 2005;**19**:1263–1276.

Grigg AP, McLachlan R, Zaja J, Szer J. Reproductive status in long-term bone marrow transplant survivors receiving busulfan-cyclophosphamide (120 mg/kg). *Bone Marrow Transplant* 2000;**26**: 1089–1095.

Hong PS, Srigritsanapol A, Chan KK. Pharmacokinetics of 4-hydroxy-cyclophosphamide and metabolites in the rat. *Drug Metab Dispos* 1991;**19**:1–7.

Horicks F, Van Den Steen G, Gervy C, Clarke HJ, Demeestere I. Both in vivo FSH depletion and follicular exposure to Gonadotrophin-releasing hormone analogues in vitro are not effective to prevent follicular depletion during chemotherapy in mice. *Mol Hum Reprod* 2018;**24**:221–232.

Howlader N, Noone AM, Krapcho M, Miller D, Brest A, Yu M, Ruhl J, Tatalovich Z, Mariotto A, Lewis DR. SEER cancer statistics review. *Natl Cancer Inst* 2019;1975–2016. 2020.

Hu J, Zhang Z, Zhao L, Li L, Zuo W, Han L. High expression of RAD51 promotes DNA damage repair and survival in KRAS-mutant lung cancer cells. *BMB Rep* 2019;**52**:151–156.

Kalich-Philosoph L, Roness H, Carmely A, Fishel-Bartal M, Ligumsky H, Paglin S, Wolf I, Kanety H, Sredni B, Meirow D. Cyclophosphamide triggers follicle activation and "burnout"; AS101 prevents follicle loss and preserves fertility. *Sci Transl Med* 2013;**5**:185ra62. ra62.

Karimian A, Mir SM, Parsian H, Refieyan S, Mirza-Aghazadeh-Attari M, Yousefi B, Majidinia M. Crosstalk between Phosphoinositide 3-kinase/Akt signaling pathway with DNA damage response and oxidative stress in cancer. *J Cell Biochem* 2019;**120**:10248–10272.

Koyama H, Wada T, Nishizawa Y, Iwanaga T, Aoki Y, Terasawa T, Kosaki G, Yamamoto T, Wada A. Cyclophosphamide-induced ovarian failure and its therapeutic significance in patients with breast cancer. *Cancer* 1977;**39**:1403–1409.

Kujjo LL, Laine T, Pereira RJG, Kagawa W, Kurumizaka H, Yokoyama S, Perez GI. Enhancing survival of mouse oocytes following chemotherapy or aging by targeting bax and Rad51. *PLoS One* 2010;**5**:e9204.

Kujjo LL, Ronningen R, Ross P, Pereira RJG, Rodriguez R, Beyhan Z, Goissis MD, Baumann T, Kagawa W, Camsari C. *et al.* RAD51 plays a crucial role in halting cell death program induced by ionizing radiation in bovine oocytes1. *Biol Reprod* 2012;**86**:76.

Kumagai K, Kubota N, Saito TI, Sasako T, Takizawa R, Sudo K, Kurokawa M, Kadowaki T. Generation of transgenic mice on an NOD/SCID background using the conventional microinjection technique. *Biol Reprod* 2011;**84**:682–688.

Lambertini M, Moore HCF, Leonard RCF, Loibl S, Munster P, Bruzzone M, Boni L, Unger JM, Anderson RA, Mehta K. *et al.* Gonadotropin-releasing hormone agonists during chemotherapy for preservation of ovarian function and fertility in premenopausal patients with early breast cancer: a systematic review and meta-analysis of individual patient–level data. *J Clin Oncol* 2018;**36**: 1981–1990.

Livak KJ, Schmittgen TD. Analysis of relative gene expression data using real-time quantitative PCR and the 2-$\Delta\Delta$CT method. *Methods* 2001;**25**:402–408.

Luan Y, Edmonds ME, Woodruff TK, Kim SY. Inhibitors of apoptosis protect the ovarian reserve from cyclophosphamide. *J Endocrinol* 2019;**240**:243–256.

Macklon NS, Fauser BCJM. Aspects of ovarian follicle development throughout life. *Horm Res* 1999;**52**:161–170.

Maidarti M, Clarkson YL, Mclaughlin M, Anderson RA, Telfer EE. Inhibition of PTEN activates bovine non-growing follicles in vitro but increases DNA damage and reduces DNA repair response. *Hum Reprod* 2019;**34**:297–307.

Maidarti M, Anderson RA, Telfer EE. Crosstalk between PTEN/PI3K/Akt signalling and DNA damage in the oocyte: implications for primordial follicle activation. *Oocyte Quality Ageing*. *Cells* 2020;**9**: 200.

Marangos P, Stevense M, Niaka K, Lagoudaki M, Nabti I, Jessberger R, Carroll J. DNA damage-induced metaphase i arrest is mediated by the spindle assembly checkpoint and maternal age. *Nat Commun* 2015;**6**:8706.

Marcozzi S, Rossi V, Salvatore G, Di Rella F, De Felici M, Klinger FG. Distinct effects of epirubicin, cisplatin and cyclophosphamide on ovarian somatic cells of prepuberal ovaries. *Aging (Albany NY)* 2019;**11**:10532–10556.

Matikainen T, Perez GI, Zheng TS, Kluzak TR, Rueda BR, Flavell RA, Tilly JL. Caspase-3 gene knockout defines cell lineage specificity for programmed cell death signaling in the ovary. *Endocrinology* 2001; **142**:2468–2480.

Meirow D, Biederman H, Anderson RA, Wallace WH. Toxicity of chemotherapy and radiation on female reproduction. *Clin Obstet Gynecol* 2010;**53**:727–739.

Meli M, Caruso-Nicoletti M, La Spina M, Nigro LL, Samperi P, D'Amico S, Bellia F, Miraglia V, Licciardello M, Cannata E. *et al.* Triptorelin for fertility preservation in adolescents treated with chemotherapy for cancer. *J Pediatr Hematol Oncol* 2018;**40**:269–276.

Nguyen QN, Zerafa N, Liew SH, Findlay JK, Hickey M, Hutt KJ. Cisplatin- and cyclophosphamide-induced primordial follicle depletion is caused by direct damage to oocytes. *Mol Hum Reprod* 2019; **25**:433–444.

Norman RJ, Buchholz MM, Somogyi AA, Amato F. hCGbeta core fragment is a metabolite of hCG: evidence from infusion of recombinant hCG. *J Endocrinol* 2000;**164**:299–305.

Orren DK, Petersen LN, Bohr VA. Persistent DNA damage inhibits S-phase and G2 progression, and results in apoptosis. *Mol Biol Cell* 1997;**8**:1129–1142.

Park BK, Park MJ, Kim HG, Han SE, Kim CW, Joo BS, Lee KS. Role of visfatin in restoration of ovarian aging and fertility in the mouse aged 18 months. *Reprod Sci* 2020;**27**:681–689.

Penny R, Olambiwonnu NO, Frasier SD. Episodic fluctuations of serum gonadotropins in pre- and post-pubertal girls and boys. *J Clin Endocrinol Metab* 1977;**45**:307–311.

Petrillo SK, Desmeules P, Truong TQ, Devine PJ. Detection of DNA damage in oocytes of small ovarian follicles following phosphoramide mustard exposures of cultured rodent ovaries in vitro. *Toxicol Appl Pharmacol* 2011;**253**:94–102.

Plo I, Laulier C, Gauthier L, Lebrun F, Calvo F, Lopez BS. AKT1 inhibits homologous recombination by inducing cytoplasmic retention of BRCA1 and RAD5. *Cancer Res* 2008;**68**:9404–9412.

Powers JF, Sladek NE. Cytotoxic activity relative to 4-hydroxycyclophosphamide and phosphoramide mustard concentrations in the plasma of cyclophosphamide-treated rats. *Cancer Res* 1983;**43**:1101–1106.

Rama RG, Prakash GJ, Krishna KM, Madan K. Meiotic spindle and zona pellucida characteristics as predictors of embryonic development: a preliminary study using PolScope imaging. *Reprod BioMed Online* 2007;**14**:166–174.

Rana S, Mohamed AR, Behnam S, Suleiman AH, Zuzana H, Moustapha H. Cyclophosphamide pharmacokinetics in mice: a comparison between retro orbital sampling versus serial tail vein bleeding. *Open Pharmacol J* 2007;**1**:30–35.

Riccetti L, Yvinec R, Klett D, Gallay N, Combarnous Y, Reiter E, Simoni M, Casarini L, Ayoub MA. Human luteinizing hormone and chorionic gonadotropin display biased agonism at the LH and LH/CG receptors. *Sci Rep* 2017;**7**:940.

Rossi V, Lispi M, Longobardi S, Mattei M, Rella FD, Salustri A, De Felici M, Klinger FG. LH prevents cisplatin-induced apoptosis in oocytes and preserves female fertility in mouse. *Cell Death Differ* 2017;**24**:72–82.

Santen RJ, Bardin CW. Episodic luteinizing hormone secretion in man. Pulse analysis, clinical interpretation, physiologic mechanisms. *J Clin Invest* 1973;**52**:2617–2628.

Shen WH, Balajee AS, Wang J, Wu H, Eng C, Pandolfi PP, Yin Y. Essential role for nuclear PTEN in maintaining chromosomal integrity. *Cell* 2007;**128**:157–170.

Sinha N, Letourneau JM, Wald K, Xiong P, Imbar T, Li B, Harris E, Mok-Lin E, Cedars MI, Rosen MP. Antral follicle count recovery in women with menses after treatment with and without gonadotropin-releasing hormone agonist use during chemotherapy for breast cancer. *J Assist Reprod Genet* 2018;**35**:1861–1868.

Sofiyeva N, Siepmann T, Barlinn K, Seli E, Ata B. Gonadotropin-releasing hormone analogs for gonadal protection during gonadotoxic chemotherapy: a systematic review and meta-analysis. *Reprod Sci* 2019;**26**:939–953.

Soleimani R, Heytens E, Darzynkiewicz Z, Oktay K. Mechanisms of chemotherapy-induced human ovarian aging: double strand DNA breaks and microvascular compromise. *Aging (Albany NY)* 2011;**3**:782–793.

Spears N, Lopes F, Stefansdottir A, Rossi V, De Felici M, Anderson RA, Klinger FG. Ovarian damage from chemotherapy and current approaches to its protection. *Hum Reprod Update* 2019;**25**:673–693.

Takai Y, Matikainen T, Jurisicova A, Kim MR, Trbovich AM, Fujita E, Nakagawa T, Lemmers B, Flavell RA, Hakem R. et al. Caspase-12 compensates for lack of caspase-2 and caspase-3 in female germ cells. *Apoptosis* 2007;**12**:791–800.

Tomari H, Honjo K, Kunitake K, Aramaki N, Kuhara S, Hidaka N, Nishimura K, Nagata Y, Horiuchi T. Meiotic spindle size is a strong indicator of human oocyte quality. *Reprod Med Biol* 2018;**17**:268–274.

Wang WH, Keefe DL. Prediction of chromosome misalignment among in vitro matured human oocytes by spindle imaging with the PolScope. *Fertil Steril* 2002;**78**:1077–1081.

Wang Y, Liu M, Johnson SB, Yuan G, Arriba AK, Zubizarreta ME, Chatterjee S, Nagarkatti M, Nagarkatti P, Xiao S. Doxorubicin obliterates mouse ovarian reserve through both primordial follicle atresia and overactivation. *Toxicol Appl Pharmacol* 2019;**381**:114714.

Watrin E, Peters JM. Cohesin and DNA damage repair. *Exp Cell Res* 2006;**312**:2687–2693.

Wei F, Yan J, Tang D, Lin X, He L, Xie Y, Tao L, Wang S. Inhibition of ERK activation enhances the repair of double-stranded breaks via non-homologous end joining by increasing DNA-PKcs activation. *Biochim Biophys Acta* 2013;**1833**:90–100.

Winship AL, Stringer JM, Liew SH, Hutt KJ. The importance of DNA repair for maintaining oocyte quality in response to anti-cancer treatments, environmental toxins and maternal ageing. *Hum Reprod Update* 2018;**24**:119–134.

Xiong B, Li S, Ai J, Yin S, OuYang Y, Sun S, Chen D, Sun Q. BRCA1 is required for meiotic spindle assembly and spindle assembly checkpoint activation in mouse oocytes1. *Biol Reprod* 2008;**79**:718–726.

Zhang T, Yan D, Yang Y, Ma A, Li L, Wang Z, Pan Q, Sun Z. The comparison of animal models for premature ovarian failure established by several different source of inducers. *Regul Toxicol Pharmacol* 2016;**81**:223–232.